Malaysian Journal of Chemistry, 2024, Vol. 26(5), 231-238
(Special Issue: *3rd Virtual International Symposium on Sciences 2023*)

Effect of Sintering Temperature on AC Susceptibility and Superconducting Properties of $(Bi_{1.6}Pb_{0.4})Sr_2CaCu_2O_8$ Superconductor

Norazimah Mohd Yusof[1], Ilhamsyah Putra Abu Bakar[2], Nurul Raihan Mohd Suib[3], Roslan Abd Shukor[4], Madihah Mujaini[2], Huda Abdullah[5], Syahrul Humaidi[6] and Nur Jannah Azman[1]*

[1]Faculty of Applied Sciences, Universiti Teknologi MARA, Cawangan Negeri Sembilan, Kampus Kuala Pilah, 72000, Kuala Pilah, Negeri Sembilan, Malaysia
[2]Center for Nuclear Energy, College of Engineering, IKRAM-UNITEN, Universiti Tenaga Nasional, 43000, Kajang, Selangor, Malaysia
[3]Pusat Asasi UiTM Kampus Dengkil, Universiti Teknologi MARA, 43800 Dengkil, Selangor, Malaysia
[4]Department of Applied Physics, Universiti Kebangsaan Malaysia 43600 Bangi, Selangor, Malaysia
[5]Centre of Advanced Electronic and Communication Engineering, Faculty of Engineering and Built Environment, Universiti Kebangsaan Malaysia, Bangi, Selangor, Malaysia
[6]FMIPA, Universitas Sumatera Utara, Jalan Biotechnology No 1, Medan 20155, Indonesia
*Corresponding author (e-mail: nurjannah@uitm.edu.my)

The effect of sintering on the structural and superconducting properties of the $(Bi_{1.6}Pb_{0.4})Sr_2CaCu_2O_8$ system has been investigated. The samples were prepared by solid-state reaction method with different sintering temperatures:820 °C, 825 °C, 830 °C, 835 °C, and 840 °C. The samples were characterized by X-ray diffraction (XRD), electrical resistance, and AC susceptibility measurement. XRD patterns showed that the Bi-2212 phase with orthorhombic unit cell was found in all samples. In general, no systematic changes in lattice parameters indicating increasing sintering temperature until 840 °C did not affect the lattice. The sample sintered at 840 °C showed the highest $T_{c\text{-onset}}$ and $T_{c\text{-zero}}$, 84 K and 71 K, respectively. The sample with the sintering temperature of 840 °C also showed the highest AC susceptibility transition temperature, $T_{c\chi'}$ (80 K). The peak temperature of the imaginary part of the susceptibility, T_p, for the sample sintered at 840 °C increased to 57 K. According to these study's findings, 840 °C is the most suitable temperature for sintering $(Bi_{1.6}Pb_{0.4})Sr_2CaCu_2O_8$ system.

Keywords: Sintering temperature; critical current density; flux pinning

Received: January 2024; Accepted: February 2024

Following the discovery of the Bi-Sr-Ca-Cu-O superconductor system, much research has been conducted to improve its superconducting properties [1-9]. It is employed in a variety of industries, including power transmission cables [10], transportation [11], nuclear fusion [12], nuclear magnetic resonance imaging [13, 14], and energy storage [15]. These are a few instances where superconducting wire and cables are used extensively. The Bi-based (Bismuth-based) HTSC (High-Temperature Superconductor) has great potential for applications in superconductor technology among the copper-oxide family of superconductors [16, 17]. It is the greatest option for superconducting HTSC [18]. Bi-based materials are industrialized and commercialized as practical materials [19, 20]. It was easily made in the forms of round wires and tapes [18, 21, 22].

The Bi-based system has three different phases, which are called Bi-(2201), Bi-(2212), and Bi-(2223), according to the number of CuO_2 layers [23]. The composition of each phase is expressed by a general formula of $(Bi, Pb)_2Sr_2Ca_{n-1}Cu_nO_x$ for n = 1, 2, 3, respectively. Each phase has a different transition temperature to the superconducting state: for n = 1 (2201) $T_c \approx 20$ K, n = 2 (2212) Tc ≈ 80 K a,nd n = 3 (2223) $T_c \approx 110$ K [24]

However, some major limitations of the Bi-based superconductor application are the intergrain weak links and weak flux pinning capability [23]. It is also difficult to obtain them in the pure phase because the Bi-2212 phase grows before the Bi-2223 phase during synthesis. The optimum temperature for 2223 phase formation was 845 °C ± 5 °C [25]. Other studies found a gradual transformation of the 2212 phase to the 2223 phase, which starts within 5 h of sintering in the air at 840 °C. Increasing the sintering temperature to 845 °C decreases the Bi-2212 phase fraction. It was also found that the Bi-2212 phase on the grain boundaries is likely to play a part in weak links, consequently reducing intergranular coupling [26].

In anticipation of the role of heat treatment conditions in improving HTSC homogeneity, this paper investigates the effect of sintering temperature

†Paper presented at the 3rd Virtual International Symposium on Sciences (3rd VISoS 2023)

on the superconductivity of polycrystalline samples of $(Bi_{1.6}Pb_{0.4})Sr_2CaCu_2O_8$. Five samples with varying sintering temperatures (820 °C, 825 °C, 830 °C, 835 °C and 840 °C) were prepared to obtain the best properties of Bi-2212. The XRD characterization was used to determine the phase. This study included measurements of electrical resistance and AC susceptibility.

EXPERIMENTAL

In the pellet form, samples of $(Bi_{1.6}Pb_{0.4})Sr_2CaCu_2O_8$ were prepared using the solid-state reaction method. Fine powders of Bi_2O_3, PbO, Sr_2CO_3, $CaCO_3$, CuO with high purity (≥99.9%) were employed. The powders were weighed and ground for 1 h. The mixed powders were calcined at 800 °C for 24 h in the air for 2 cycles with 1 h of grindings before the second calcination. Then, they were taken out from the furnace and re-ground. Following this, 2.5 g of the powders were pressed at 5 tons into pellets of 12.5 mm diameter and 2 mm thickness. The pellets were placed in the furnace and sintering was carried out at 820 °C, 825 °C, 830 °C, 835 °C and 840 °C for 50 h. The XRD characterization identified the samples' phase using a Bruker D8 Advance X-ray diffractometer.

The electrical resistance measurements were determined using the standard four-point-probe DC method with silver paste for electrical contacts. The experimental set-up consisted of a closed cycle refrigerator from CTI Cryogenics (model 22), a temperature controller from LakeShore (model 325), a multimeter (Keithley 197), and a constant current source (Keithley220). $T_{c\ zero}$ is the temperature at which the electrical resistance drops to zero. The onset of superconductivity, $T_{c\ onset,}$ was taken as the temperature at which the tangent of the resistance versus temperature curve intersects with the tangent of the part where resistance dropped precipitously.

An AC susceptometer from Cryo Industry model number REF-1808-AS was used to measure the complex susceptibility, $\chi = \chi' + i\chi''$, where c' is the real part and c" is the imaginary part. The frequency used was 295 Hz, and the applied magnetic field was $H = 5$ Oe. The Bean's model [27] was used to calculate the critical current density at the peak temperature, of c", T_p with formula $J_c(T_p) = H_c / (lw)^{1/2}$ where H is the applied field, l and w are the dimensions of the cross-section of the bar shape sample.

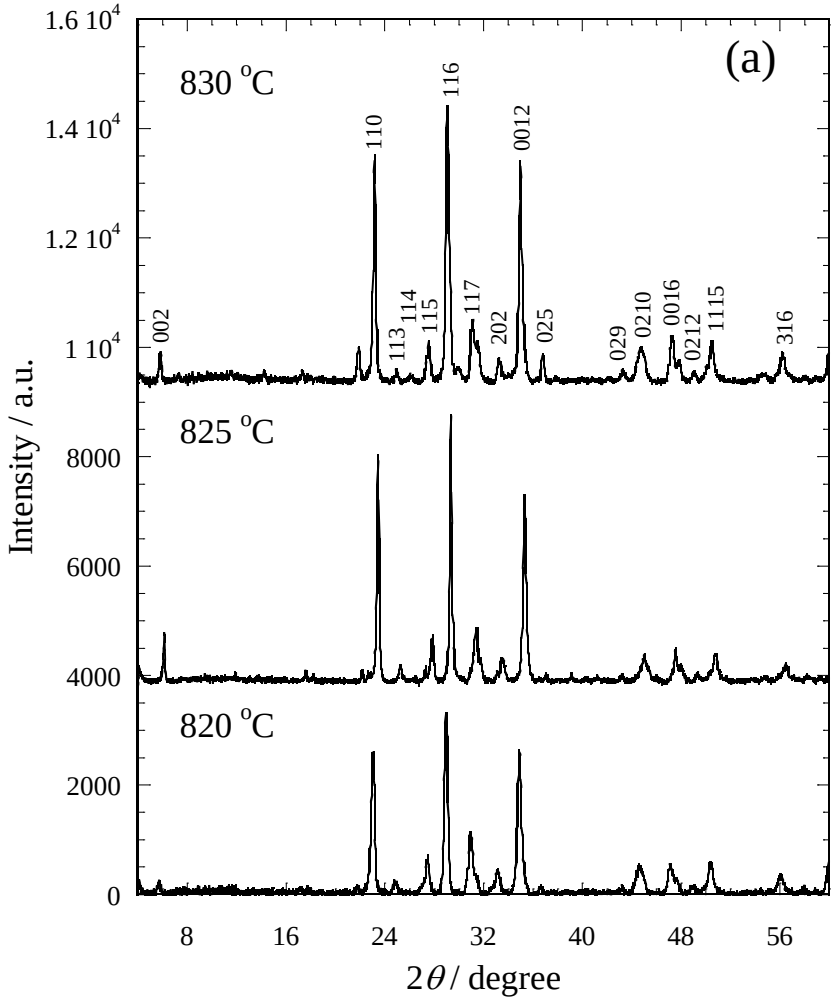

Figure 1 (a). X-ray diffraction patterns of $(Bi_{1.6}Pb_{0.4})Sr_2CaCu_2O_8$ sintered at 820, 825 and 830 °C.

RESULTS AND DISCUSSION

XRD pattern of $(Bi_{1.6}Pb_{0.4})Sr_2CaCu_2O_8$ with sintering temperatures 820 °C, 825 °C, 830 °C, 835 °C and 840 °C are shown in Figure 1 (a) and Figure 1 (b). The Bi-2212 phase with orthorhombic unit cell was found in all samples. The first peak at $2\theta \sim 5.7°$ (002) corresponds to the signature peak of the Bi-2212 phase [28], which can be observed clearly. The Bi-2212 peaks can be seen to appear with increasing temperature gradually.

The sample with the sintering temperature of 820 °C showed lattice parameters a = 5.479 Å, b = 5.361 Å and c = 30.765Å (Table 1). In general, no systematic changes in the lattice parameters *a, b, and c* were observed with increasing sintering temperature. With a sintering temperature of up to 840 °C, all samples exhibited a dominant Bi-2212 phase. However, even no systematic change in the lattice parameter, V is slightly increase from 903.7 $Å^3$ to 904.3 $Å^3$.

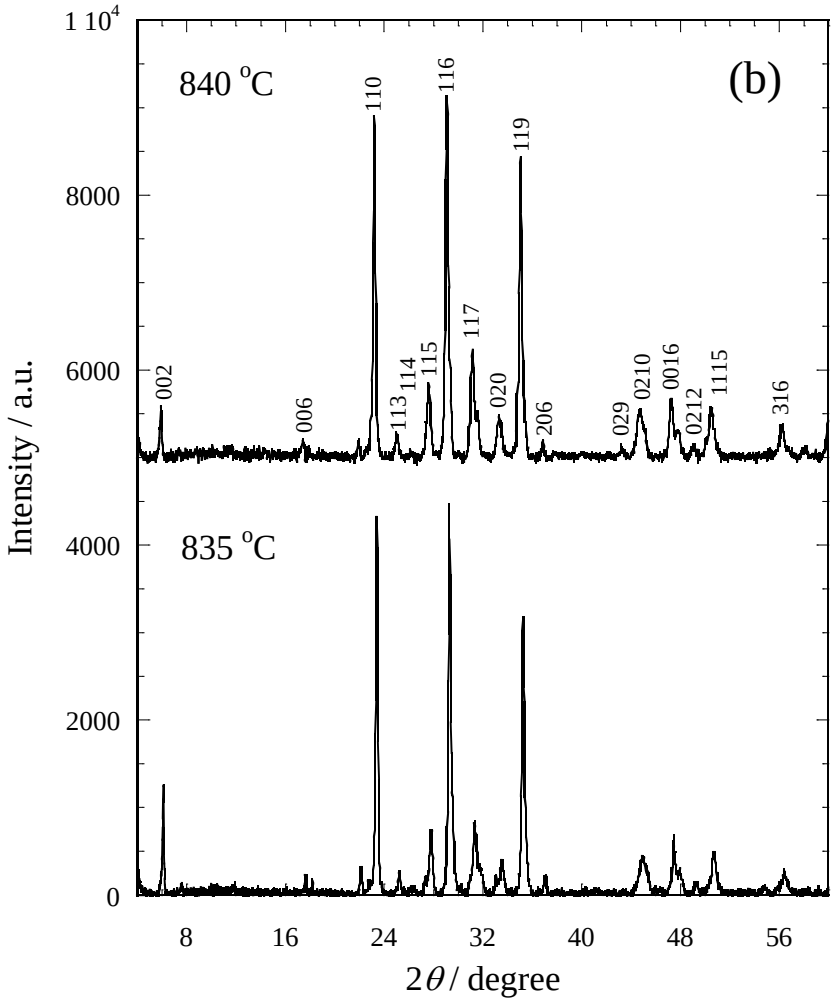

Figure 1 (b). X-ray diffraction patterns of $(Bi_{1.6}Pb_{0.4})Sr_2CaCu_2O_8$ sintered at 835 and 840 °C.

Table 1. $T_{c\text{-onset}}$, $T_{c\text{-zero}}$, ΔT_c, $T_{c\chi'}$, T_p, $J_c(T_p)$, $\rho_{297\,K}$, lattice parameters for Bi-2212 phase of $(Bi_{1.6}Pb_{0.4})Sr_2CaCu_2O_8$ for 820, 825, 830, 835 and 840 °C

Sintering Temperature /°C	$T_{c\text{-onset}}$ /K	$T_{c\text{-zero}}$ /K	ΔT_c /K	$T_{c\chi'}$ /K	T_p /K	$J_c(T_p)$ /A cm^{-2}	ρ_{297K} /mΩ-cm	a /Å	b /Å	c /Å	V /Å^3
820	80	70	10	74	56	20	2.85	5.479	5.361	30.765	903.7
825	77	64	13	73	56	18	3.31	5.416	5.396	30.853	901.7
830	80	70	10	79	< 20	26	2.42	5.461	5.363	30.794	902.0
835	83	63	20	79	< 20	19	6.80	5.408	5.391	31.045	905.0
840	84	71	13	80	57	16	2.20	5.469	5.375	30.767	904.3

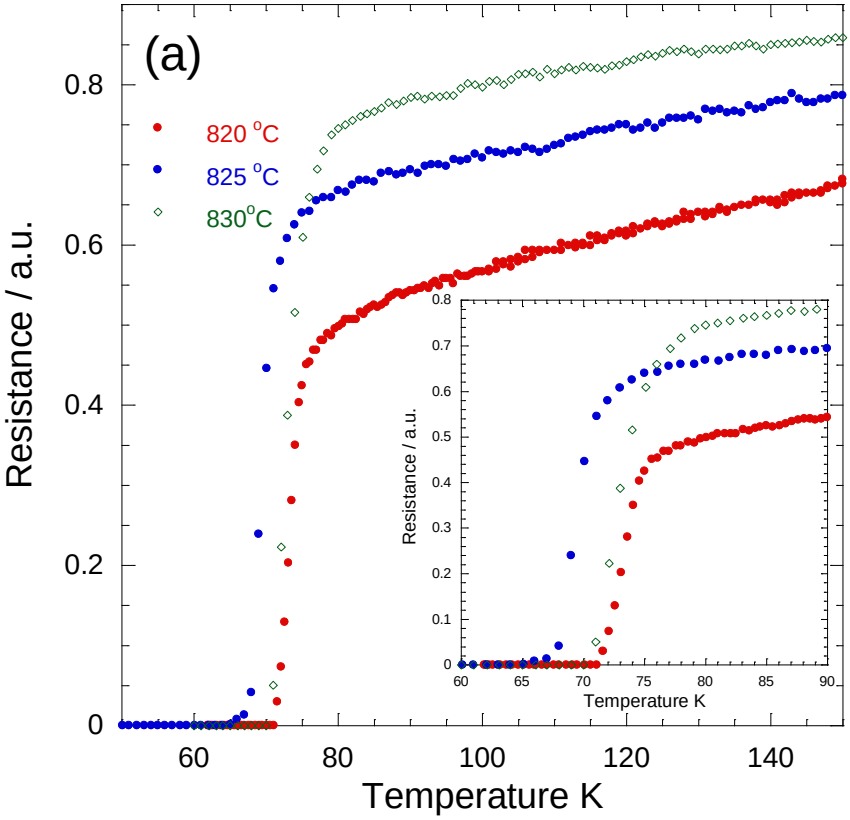

Figure 2 (a). Electrical resistance versus temperature of $(Bi_{1.6}Pb_{0.4})$ $Sr_2CaCu_2O_8$ sintered at 820, 825 and 830 °C.

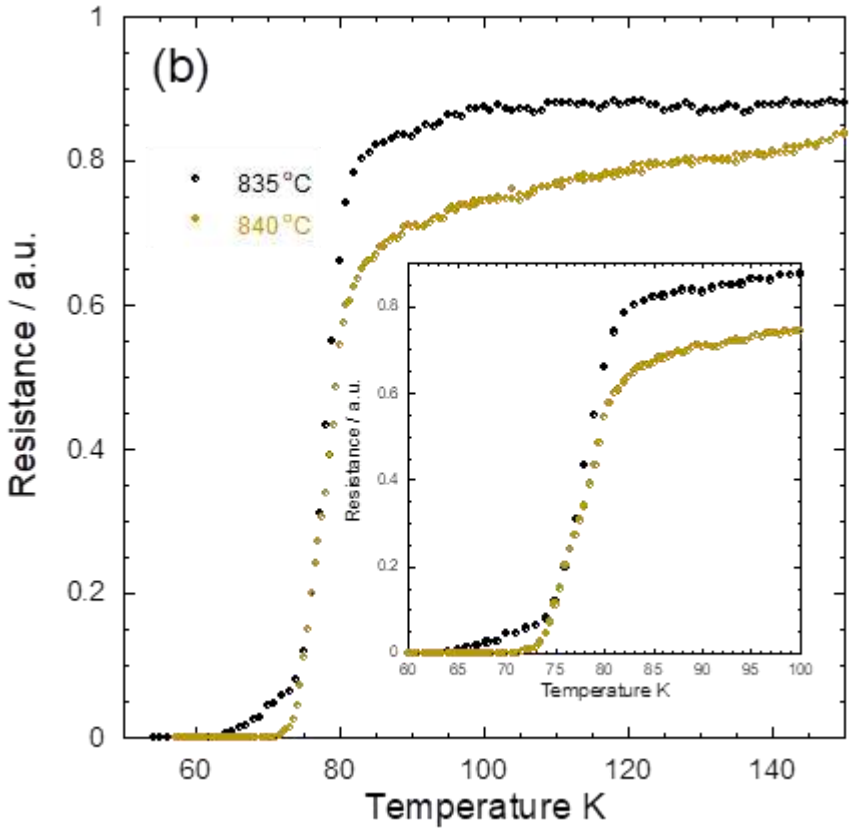

Figure 2 (b). Electrical resistance versus temperature of $(Bi_{1.6}Pb_{0.4})Sr_2CaCu_2O_8$ sintered at 835 and 840 °C.

Figure 2(a) shows the normalized electrical resistance versus temperature curves. The curves showed metal-like behaviour in the normal state. Impurity phases can lead to a *tail* in the resistance versus temperature curves. Regarding the resistance measurement's outcomes at room temperature, $(Bi_{1.6}Pb_{0.4})$ $Sr_2CaCu_2O_8$ exhibits metallic properties after sintering for 820 °C – 840 °C with value ρ_{297K} = 2.85 mΩ-cm – 6.8 mΩ-cm. The resistance property at room temperature is done to estimate the properties of the sample before cooling the sample.

Figure 2(b) as shown by the Bi-2212 samples which were heated for only 48 hours in the final heating stages. The sintering temperatures of 820 °C and 830 °C had little effect on $T_{c\text{-onset}}$, $T_{c\text{-zero}}$ and ΔT_c. The sample sintered at 840 °C showed the highest $T_{c\text{-onset}}$ and $T_{c\text{-zero}}$ which are 84 K and 71 K, respectively. All the samples show zero electrical resistance $T_{c\text{-zero}}$ within the range of 70 to 71 K and $T_{c\text{-onset}}$ is between 80 and 84 K (Table 1). The sample with the sintering temperature of 835 °C showed a large transition width, ΔT_c which could be attributed to the large variation of the transition temperature of individual Bi-2212 superconducting grains. The broad transition width, ΔT_c indicated the inhomogeneities in the individual superconducting grains.

The AC susceptibility versus temperature curves are shown in Figure 3 (a) and Figure 3 (b). The transition temperature, $T_{c\chi'}$, is indicated by the sudden decrease in the real part of the susceptibility χ'. $T_{c\chi'}$ indicates diamagnetic shielding which marks the onset transition temperature of bulk superconductivity. The sample with the sintering temperature of 840 °C showed the highest $T_{c\chi'}$ (80 K). Two peaks representing the AC losses should be observed in the imaginary part, χ'' of susceptibility. The narrower peak at higher temperature is caused by intrinsic losses (intragrain coupling) and a broader peak at low temperature is due to intergrain coupling losses. However, in our experiments, no intrinsic peaks were observed in all samples due to the low applied field (H_{ac} = 5 Oe)

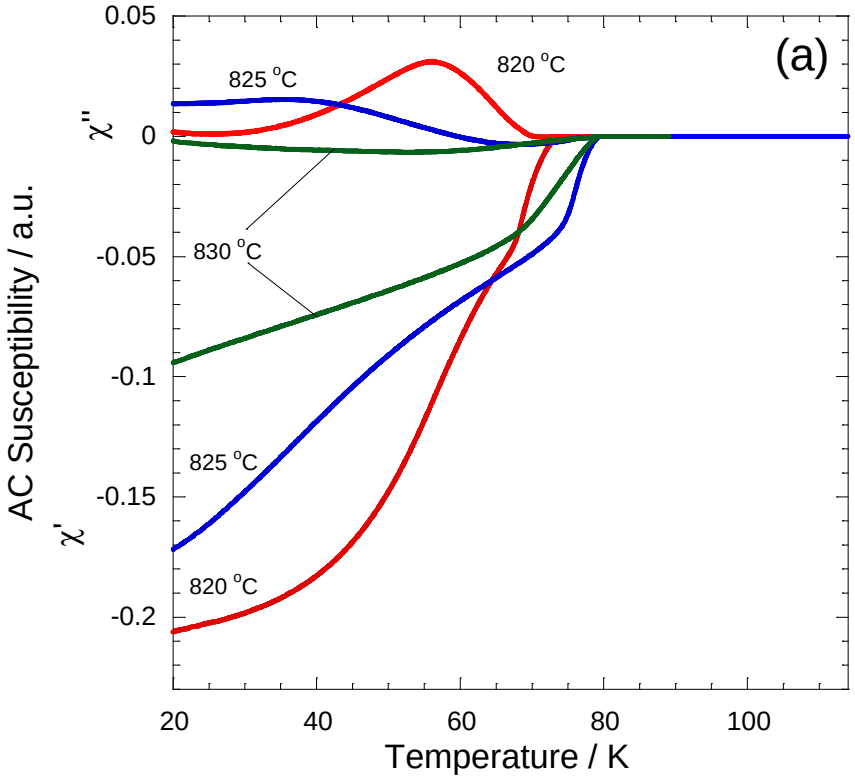

Figure 3 (a). AC Susceptibility of $(Bi_{1.6}Pb_{0.4})Sr_2CaCu_2O_8$ sintered at 820, 825 and 830 °C.

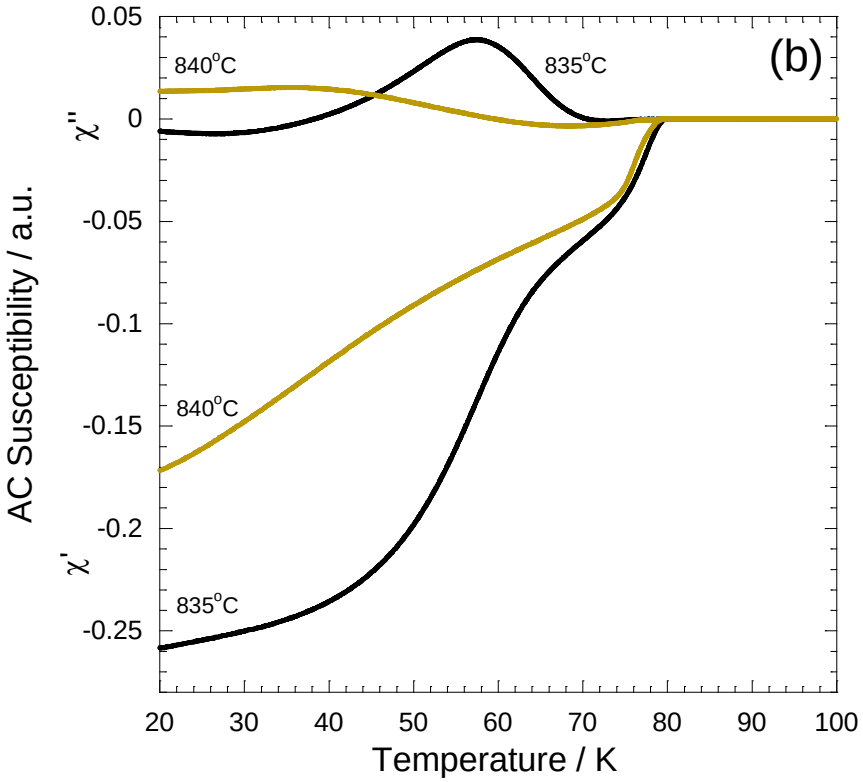

Figure 3 (b). AC Susceptibility of $(Bi_{1.6}Pb_{0.4})Sr_2CaCu_2O_8$ sintered at 835 and 840 °C.

The peak temperature T_p in the imaginary part of the susceptibility χ'' represents AC losses. The peak temperature of the imaginary part of the susceptibility T_p shows the temperature where there is full flux penetration of the grains. The weaker the pinning, the larger the T_p was shifted to a lower temperature. Below T_p, the amplitude of χ'' falls due to the decrease in flux penetration. T_p shifts to higher temperatures if the flux pinning force is increased. At T_p, the intergrain currents arrive at the value allowing the AC field to penetrate through the intergrain space to the sample centre [29]. The increasing sintering temperature, for the sample with the sintering temperature of 820 °C to 825 °C does not affect the T_p value, it remains at 56 K. T_p for the sample with the sintering temperature of 840 °C was increased to 57 K. This indicated that sintering temperature improved the flux pinning as shown by the shift in T_p for 840 °C temperatures compared to 820 °C sample. The increase in T_p can be attributed to better grain connectivity. The critical current density J_c at the peak temperature T_p of χ'' was calculated using the Bean model formula $J_c(= H_a/ab)^{1/2}$ where a and b are the size of the cross-section of the bar-shaped sample. $J_c(T_p)$ represents the current density for flux penetration at T_p while J_c represents the transport current between grains in the samples. The transport critical current density at the peak temperature $J_c(T_p)$ was around 16.0–20.0 A cm^{-2} (Table 1).

CONCLUSION

Based on this work, it is determined that the formation of the Bi-2212 phase is temperature-dependent. A sintering temperature of 840 °C for 48 h improved the flux pinning and grain connectivity. Sintering also enhances the superconducting grains coupling characteristic and homogenises the superconducting phases, both of which result increase T_c. Sintering at 840 °C results in the highest $T_{c\text{-onset}}$ value of 80 K. However, it has no effect on the lattice properties at this temperature to the Bi-2212 phase. Making it the most suitable temperature for sintering to obtain the Bi-2212 phase.

ACKNOWLEDGEMENTS

The authors thank Universiti Teknologi MARA 600-RMC/GIP 5/3 (103/2023) and (600-KNS (PJI(CRSF .5/3 (01/2022) for the funding.

REFERENCES

1. Özçelik, B., Ergin, I., Madre, M. A. & Sotelo, A. (2020) Effect of rubidium substitution on the physical and superconducting properties of textured high-Tc BSCCO samples. *Journal of Superconductivity and Novel Magnetism*, **33**, 1285–1292.

2. Gayathri, V., Sathyanarayana, A. T., Amaladass, E. P., Vinod, K., Kumary, T. G., Pandian, R. & Mani, A. (2021) Evolution of superconducting properties of coexistent Bi-2212 and Bi-2223 phases in BSCCO.

3. Kavitha, M., Sarvesh, S., Arshad, M., Surendar, M. & Ragavan, G. (2024) Effect of Ba and Mg Substitution on the Phase Formations of Combustion Synthesized BSCCO Superconductor. *Journal of The Institution of Engineers (India): Series D*, 1–7.

4. Jassim, A. K. & Abbas, M. M. (2021) Superconductivity of BSCCO Compound Substituted Partially by Zr Nanoparticles at Bi Site. In *Journal of Physics: Conference Series*, *IOP Publishing*, **2114**, 1, 012065, December, 2021.

5. Belala, K., Galluzzi, A., Mosbah, M. F. & Polichetti, M. (2021) Transport and magnetic properties of Bi (Pb) 2212 superconducting ceramics doped by low rate of potassium. *Materials Science-Poland*, **39(1)**, 15–23.

6. Siregar, D. R. D., Yudanto, S. D., Chandra, S. A., Lubis, E. F. R., Humaidi, S. & Darsono, N. (2021) Improvement of the superconducting properties of carbon addition on $Bi_{1.6}Pb_{0.4}Sr_2Ca_2Cu_3O_{10+\delta}$ prepared through the two-step sintering process. *Journal of Metals, Materials and Minerals*, **31(4)**, 76–81.

7. Chen, Y., Shao, L., Zhao, G., Liu, Q., Huang, Y., Liu, Z. & Zheng, B. (2022) Optimization for preparing Bi1. 68Pb0. 32Sr1. 75Ca1. 85Cu2. 85O10+ y powders by wet ball milling. *Materials Research Express*, **9(6)**, 066002.

8. Wei, K., Ing, K. & Abd-Shukor, R. Superconducting and Transport Properties FeF_2 Added $YBa_2Cu_3O_{7-\delta}$ Superconductor.

9. Yu, Y., Ma, L., Cai, P., Zhong, R., Ye, C., Shen, J. & Zhang, Y. (2019) High-temperature superconductivity in monolayer $Bi_2Sr_2CaCu_2O_{8+\delta}$. *Nature*, **575(7781)**, 156–163.

10. Slimani, Y. & Hannachi, E. (2022) Fabrication Technologies of Superconducting Cables and Wires. In Superconducting Materials: Fundamentals, Synthesis and Applications. *Singapore: Springer Nature Singapore*, 271–299.

11. Bhullar, M., Sagwal, A. & Agrawal, P. (2022) Superconductor on wheels. In *AIP Conference Proceedings AIP Publishing*, **2520**, 1, August 2022.

12. Haack, J. (2024) Superconductivity for Nuclear Fusion: Past, Present, and Future. *Arabian Journal for Science and Engineering*, 1–5.

13. Yanagisawa, Y., Hamada, M., Hashi, K. & Maeda, H. (2022) Review of recent developments in ultra-high field (UHF) NMR magnets in the Asia region. *Superconductor Science and Technology*, **35(4)**, 044006.

14. Piao, R., Miyoshi, Y., Yoshikawa, M., Saito, K., Hamada, M., Matsumoto, S. & Yanagisawa, Y. (2019) Design and development of a compact 1 GHz (23.5 T)-class NMR magnet with Bi-2223 inner coils. *IEEE Transactions on Applied Superconductivity*, **29(5)**, 1–7.

15. Adetokun, B. B., Oghorada, O. & Abubakar, S. J. A. (2022) Superconducting magnetic energy storage systems: Prospects and challenges for renewable energy applications. *Journal of Energy Storage*, **55**, 105663.

16. Hasan, M. S. & Ali, S. S. (2022) High Temperature Superconductors: Materials and Applications. *Superconductors: Materials and Applications*, **132**, 179–193.

17. Koblischka-Veneva, A. & Koblischka, M. R. (2022) High-T c Cuprate Superconductors: Materials, Structures and Properties. In *Superconducting Materials: Fundamentals, Synthesis and Applications, Singapore: Springer Nature Singapore*, 181–209.

18. Shen, T. & Garcia Fajardo, L. (2020) Superconducting accelerator magnets based on high-temperature superconducting Bi-2212 round wires. *Instruments*, **4(2)**, 17.

19. Hayashi, K. (2020) Commercialization of Bi-2223 superconducting wires and their applications. *Sei Tech. Rev*, **91**, 68–74.

20. Yao, C. & Ma, Y. (2021) Superconducting materials: Challenges and opportunities for large-scale applications. *Iscience*, **24(6)**.

21. Tang, Y., Xu, Y., Yan, S., Feng, F. & Yan, G. (2022) Superconducting Wires and Tapes for SMES. Advances in Energy Storage: Latest Developments from R&D to the Market, 149–164.

22. Jusoh, M. M. (2021) Kerentanan arus ulang alik dan sifat elektrik superkonduktor suhu tinggi bi1. 6pb0. 4sr2cacu2o8 dengan penambahan logam sulfida (CdS, PbS, ZnS, FeS dan MoS2) (Doctoral dissertation, UKM, Bangi).

23. Ghahfarokhi, S. M. & Shoushtari, M. Z. (2010) Structural and physical properties of Cd-doped Bi1. 64Pb0. 36Sr2Ca2− xCdxCu3Oy superconductor. *Physica B: Condensed Matter*, **405(22)**, 4643–4649.

24. Muralidhar, M., Satyavathi, S., Babu, V. H., Pena, O. & Sergent, M. (1993) Effect of Ca2PbO4 on the formation of the (2223) phase in the Bi Pb Sr Ca Cu O system. *Materials Science and Engineering: B*, **20(3)**, 312–317.

25. Chen, Y. L. & Stevens, R. (1992) 2223 phase formation in Bi (Pb)─ Sr─ C─ a─ Cu─ O: II, the role of temperature—reaction mechanism. *Journal of the American Ceramic Society*, **75(5)**, 1150–1159.

26. Kameli, P., Salamati, H. & Eslami, M. (2006) The effect of sintering temperature on the intergranular properties of Bi2223 superconductors. *Solid state communications*, **137(1-2)**, 30–35.

27. Bean, C. P. (1964) Magnetization of high-field superconductors. *Reviews of modern physics*, **36(1)**, 31.

28. Masnita, M. J. & Abd-Shukor, R. (2020) Iron sulfide effects on AC susceptibility and electrical properties of $Bi_{1.6}Pb_{0.4}Sr_2CaCu_2O_8$ superconductor. *Results in Physics*, **17**, 103177.

29. Gömöry, F. (1997) Characterization of high-temperature superconductors by AC susceptibility measurements. *Superconductor Science and Technology*, **10(8)**, 523.